Electronic Supplementary Information

Combining cooperativity with sequestration: a novel strategy for discrimination of single nucleotide variants

Shichao Hu, Na Li and Feng Liu*

Beijing National Laboratory for Molecular Sciences, Key Laboratory of Bioorganic Chemistry and Molecular Engineering of Ministry of Education, College of Chemistry and Molecular Engineering, Peking University, Beijing 100871, China.
* Corresponding author. E-mail: liufeng@pku.edu.cn

Materials and Reagents

Synthetic DNA oligonucleotides and 2×PCR Master Mix were purchased from Sangon Inc. (Shanghai, China). The DNA oligonucleotide sequences are provided in Table S1 and S2. The DNA sequences were dissolved in TE buffer solution (50 mM tris(hydroxymethyl)aminomethane (Tris) and 1 mM ethylenediaminetetraacetic acid (EDTA); pH 8.0) and stored at 4 ^{o}C.

Native Polyacrylamide Gel Electrophoresis Experiments

The polyacrylamide gel electrophoresis (PAGE) samples were prepared in steps. First, before the addition of the PM and the MM, the SR and SR+SEQ mixed solutions were prepared according to the final concentrations of 4 μM SR, 10 μM SEQ, 8 μM PM and 8μM MM. Then the mixed solutions were heated at 53℃ for 5 min and naturally cooled down to room temperature. Afterwards, appropriate amounts of PM and MM were added into the sample, and waited for 20 min to allow the reaction to take place. Then appropriate amounts of SYBR Green I and 5X loading buffer were added to reach their working concentrations. After that, 15% native PAGE experiments were carried out at 110 V in 1X TBE buffer (90 mM Tris, 90 mM boric acid, 2 mM EDTA; pH 8.0) for 70 min. Images were taken in a Tanon 1600 imager (Tanon, China) using a Canon 9301S camera (Canon, Japan).

Fluorescence Measurements

Fluorescence measurements were performed by using an F-7000 fluorescence spectrophotometer (Hitachi, Japan) with a water-bath circulator to maintain the

temperature. Sample solutions were excited at 495 nm with a slit size of 10 nm, and the emission signal was recorded at 520 nm with a slit size of 10 nm (in the experiments about SR duplex probe concentration robustness, the excitation and emission slit sizes of 5 nm were used when the probe concentration was larger than 100 nM to avoid photo detector saturation).

For preparation of the mixed solution containing the SR and the SEQ, the substrate strand, the reporter strand, and the SEQ were mixed together in TNM buffer solution (50 mM Tris, 100 mM NaCl and 5 mM $MgCl_2$; pH 7.5) at final concentrations of 20 nM SR and 300 nM SEQ. The resulting solutions were heated by boiling water bath for 3 min and then naturally cooled down to room temperature. 300 μL mixed solution containing the SR and the SEQ was used in each measurement.

The mixed solution containing the SR and the SEQ was put in the cuvette, and incubated in the F-7000 fluorescence spectrophotometer for about 10 min to allow temperature equilibration. Then the fluorescence data was recorded for 20 s to obtain the base line. Afterwards, 2 μL target solution was added into the cuvette and mixed quickly within 20 s, then the fluorescence data was continuously recorded for about 30 min.

Detection of *KRAS* Mutation in PCR Amplicons

To a 200 μL PCR tube, 44 μL water, 50 μL 2×PCR Master Mix, 2 μL forward primers (0.8 pmol), 2 μL reverse primers (40 pmol), and 2 μL mixed ssDNA templates (total amount 2 fmol, 53 pg) (see Table S2 for DNA oligonucleotide sequences) were added and mixed well. PCR procedure (94.0 ^{o}C for 30 s, 57.5 ^{o}C for 20 s, 72.0 ^{o}C for 30 s, 30 cycles) was performed by using a DNA Engine Opticon 2 (MJ Research, USA). After the PCR amplification, 5 μL (0.25 nmol) Opener1 and 5 μL (0.25 nmol) Opener2 were added to the amplicons respectively to unwind the secondary structure. The fluorescence data was measured following the same procedure described in "Fluorescence Measurements" except using 100 μL of PCR products after addition of Opener1 and Opener2 instead of 2 μL target solution.

Table S1 DNA oligonucleotide sequences used in exploring performance of the SNV discrimination systems.

Name	Sequence (from 5' to 3')
Sub-A	CTTCACACTCTACCTCTACCCTT(BHQ-1)CTTCACACTCTACCTCTACCCT
Rep-T6-A	GAGGTAGAGTGTGAAGT(6-FAM)AGGGTAGAGGTAGAGT
Sub-T	CTTCACACTCAACCTCTACCCTT(BHQ-1)CTTCACACTCAACCTCTACCCT
Rep-T6-T	GAGGTTGAGTGTGAAGT(6-FAM)AGGGTAGAGGTTGAGT
Sub-C	CTTCACACTCGACCTCTACCCTT(BHQ-1)CTTCACACTCGACCTCTACCCT
Rep-T6-C	GAGGTCGAGTGTGAAGT(6-FAM)AGGGTAGAGGTCGAGT
Rep-T5-C	AGAGGTCGAGTGTGAAGT(6-FAM)AGGGTAGAGGTCGAGTG
Rep-T7-C	AGGTCGAGTGTGAAGT(6-FAM)AGGGTAGAGGTCGAG
Sub-G	CTTCACACTCCACCTCTACCCTT(BHQ-1)CTTCACACTCCACCTCTACCCT
Rep-T6-G	GAGGTGGAGTGTGAAGT(6-FAM)AGGGTAGAGGTGGAGT
SEQ-A	CGGCGG-ACACTCTACCTCT-CCGCCG
SEQ-T	CGGCGG-ACACTCAACCTCT-CCGCCG
SEQ-C	CGGCGG-ACACTCGACCTCT-CCGCCG
SEQ-G	CGGCGG-ACACTCCACCTCT-CCGCCG
SEQ-A-5CG	GGCGG-ACACTCTACCTCT-GGCGG
SEQ-A-7CG	CGGCCGG-ACACTCTACCTCT-CGGCCGG
Classic-Sub-A	CTTCACACTCTACCTCTACCCTT(BHQ-1)
Classic-Rep-A	T(6-FAM)AGGGTAGAGGTAGAGT
Classic-Sub-T	CTTCACACTCAACCTCTACCCTT(BHQ-1)
Classic-Rep-T	T(6-FAM)AGGGTAGAGGTTGAGT
Classic-Sub-C	CTTCACACTCGACCTCTACCCTT(BHQ-1)
Classic-Rep-C	T(6-FAM)AGGGTAGAGGTCGAGT
Classic-Sub-G	CTTCACACTCCACCTCTACCCTT(BHQ-1)
Classic-Rep-G	T(6-FAM)AGGGTAGAGGTGGAGT

Table S2 DNA oligonucleotide sequences used in the detection of *KRAS* G12D (c.35G>A) mutation.

Name	Sequence (from 5' to 3')
Sub-*KRAS*-A	GCCTACGCCATCAGCTCCAACTT(BHQ-1)GCCTACGCCATCAGCTCCAACT
Rep-*KRAS*-A	AGCTGATGGCGTAGGCT(6-FAM)AGTTGGAGCTGATGGC
SEQ-wild-type	CGGCGG-ACGCCACCAGCTC-CCGCCG
Wild-type	GCCTGCTGAAAATGACTGAATATAAACTTGTGGTAGTTGGAGCTGGTGGC GTAGGCAAGAGTGCCTTGACGATACAGCTAA
Mutant-type	GCCTGCTGAAAATGACTGAATATAAACTTGTGGTAGTTGGAGCTGATGGC GTAGGCAAGAGTGCCTTGACGATACAGCTAA
Forward primer	TTAGCTGTATCGTCAAGGCACTC

Reverse primer	GCCTGCTGAAAATGACTGAATATA
Opener1	ACCACAAGTTTATATTCAGTCATTTTCAGCAGGC
Opener2	TTAGCTGTATCGTCAAGGCACTCTT

Table S3 Comparison between the proposed SNV discrimination strategy combining cooperativity and sequestration with other SNV discrimination approaches reported since 2014.[a]

Discrimination format	Discrimination Factor (DF)	Reference
Enzyme-free approach		
SNV discrimination strategy combining cooperativity with sequestration	67–618, median=194 (12 substitutions)	This work
Electrochemical biosensor using electrospun fibres with polyanionic grafts	~22 (T>A substitution)[b] ~37 (G>C substitution)[b]	1
Mismatched stacking circuits	~2.5 (G>U)[b]	2
Silver nanoparticle coupled directional fluorescence spectrometry	28 (A>T substitution)	3
Toehold-mediated strand displacement involving the ethidium bromide intercalator	1.1–8095, median=2.8 (12 substitutions)	4
Dynamic sandwich assay on magnetic beads	393 (G>A substitution)	5
Kinetic discrimination by localized surface plasmon resonance	<2[b] (A>C substitution)	6
Sequestration-assisted molecular beacon	12–1144, median=117 (20 SNMs)[c]	7
Discrimination by competition and catalytic amplification	23 (A>G substitution)	8
X-probe based toehold-mediated strand displacement	2.0–20[b] (11 SNVs)	9
Three-dimensional nanotip sensing array	26[b] (T>C substitution)	10
Piezoelectric plate sensor coated with a locked nucleic acid probe	~5.8 (A>C substitution)	11
Sandwich hybridization on magnetic beads	3.2 (G>A substitution)	12
Spontaneous cascade DNA branch migration	7.8–17.9, median=12 (3 SNVs)	13
Energy driven cascade recognition	45–109, median=70 (6 SNMs)[c]	14
Gapped-duplex-based approach	62–225[b] (3 SNVs)	15
Enhanced solid-phase hybridization	5[b] (A>C substitution)	16
Switchable lanthanide luminescence binary probes	~0.9–1400, median between 10–20 (15 SNVs)	17
DNA–streptavidin dendrimer amplified sensing platform	17–72 (3 SNVs)	18
Enhanced destabilization of mismatched	3.8–5.2 (4 SNVs)	19

DNA using gold nanoparticles		
Simulation-guided DNA probe and sink design	Median β =890[d] (44 SNVs)	20
Protected DNA strand displacement	3.6–2×10^3, median=26.4 (12 SNVs)	21
DNA–gold nanoparticle probe-fueled DNA strand displacements	5.6–58[b] (18 SNMs)[c]	22
Adenosine-based molecular beacon	7.5–10[b] (3 SNVs)	23
Locked nucleic acid-integrated with toehold-mediated strand displacement	29[b] (G>T substitution)	24
G-rich hairpin probes	1.7–8.9[b] (3 SNVs)	25
Blocker-enhanced hybridization	9.6–36[b] (6 SNVs)	26
Controller DNA technology	>100 (6 SNVs)	27
Gold nanoparticle-conducted DNA bioarrays	6.8–19.7 (12 SNVs)	28
Optimizing temperature hybridization	~1.4[b] (G>T substitution)	29
DNA-fueled molecular machine	68–137[b] (5 SNMs)[c]	30
Enhanced DNA toehold exchange reaction	14–42[b] (19 SNMs)[c]	31
Enzyme approach		
Two-stage amplification reaction using molecular beacons as turn-on probes	~2.9 (G>C substitution)[b]	32
CRISPR/Cas9 triggered isothermal exponential amplification reaction	6.5 (G>C substitution)	33
Nucleic acid self-assembly circuitry aided by exonuclease III	33 (T>A substitution) 44 (C>A substitution)	34
Surface acoustic wave biosensor synergizing DNA-mediated *in situ* silver nanoparticle growth	3.9 (A>T substitution)[b]	35
Endonuclease IV based competitive DNA probe assay	510–1079 (3 C>X substitutions)	36
Multiplexed enrichment of rare DNA variants via sequence-selective and temperature-robust amplification	1000-fold enrichment	37
Droplet-based microfluidic platform for kinetics-based detection of single nucleotide variation	100–550 (6 SNVs)	38
Discrimination cascade	median=491 (14 SNMs)[c]	39
Branch-migration based fluorescent probe	10–311, median=127 (9 SNVs)	40
Controllable mismatched ligation	6.8–42[b] (12 SNVs)	41
Strand displacement and selective digestion	50.2–970, median=95.7 (15 SNVs)	42
Nicking endonuclease assisted target recycling and hyperbranched rolling circle	~4.8 (C>A substitution)	43

amplification		
5'-abasic lesion enhanced isothermal ligase chain reaction	7–12 (3 SNVs)	44
Ligation chain reaction	13[b] (C>A substitution)	45
Nicking endonuclease-assisted target recycling and magnetic nanoparticle separation	~4[b] (A>G substitution)	46
Abasic site modified fluorescent probe and lambda exonuclease	158–902, median=499 (9 SNVs)	47
Lambda exonuclease and a chemically modified DNA substrate structure	4.0–320, median=30 (12 SNVs)	48
T7 exonuclease digestion with target cyclic amplification	26 (C>T substitution)	49
Binding-induced DNA nanomachine	~5.9 (G>A substitution)	50
Specific amplification using variants of a *thermus aquaticus* DNA polymerase	1485 (G>A substitution)	51
Hybridization assay with ligation-mediated amplification	3.8–28[b] (4 SNVs)	52
Rolling circle amplification combined with gold nanoparticles-aptamer labeling	27 (G>C substitution)	53
G-quadruplex based two-stage isothermal exponential amplification	5.1[b] (C>G substitution)	54
Toehold-mediated strand displacement triggered isothermal DNA amplification	7.5–12.4 (3 SNVs)	55

[a]Not including the works from which we cannot obtain DFs. Updated on the basis of Table S3 in our previously reported work.[7]

[b]Calculated from data supplied in the articles.

[c]Including insertion and deletion.

[d]β is defined as the normalized fold-change, which is not identical to DF.

References

1 T. E. Kerr-Phillips, N. Aydemir, E. W. C. Chan, D. Barker, J. Malmström, C. Plesse and J. Travas-Sejdic, *Biosens. Bioelectron.*, 2018, **100**, 549–555.

2 W. Cheng, Y. Zhang, H. Yu, W. Diao, F. Mo, B. Wen, W. Cheng and Y. Yan, *Sens. Actuators B Chem.*, 2018, **255**, 3298–3304.

3 J. Chen, Z. Luo, Y. Wang, Z. Huang, Y. Li and Y. Duan, *Sens. Actuators B Chem.*, 2018, **255**, 2306–2313.

4 R. A. Fenati, A. R. Connolly and A. V. Ellis, *Anal. Chim. Acta*, 2017, **954**, 121–128.

5 J. Wang, G. Xiong, L. Ma, S. Wang, X. Zhou, L. Wang, L. Xiao, X. Su and C. Yu, *Biosens. Bioelectron.*, 2017, **94**, 305–311.

6 A. Rapisarda, N. Giamblanco and G. Marletta, *J. Colloid Interface Sci.*, 2017, **487**, 141–148.

7 S. Hu, W. Tang, Y. Zhao, N. Li and F. Liu, *Chem. Sci.*, 2017, **8**, 1021–1026.

8 S. X. Chen and G. Seelig, *J. Am. Chem. Soc.*, 2016, **138**, 5076–5086.

9 X. Chen, D. Zhou, H. Shen, H. Chen, W. Feng and G. Xie, *Sci. Rep.*, 2016, **6**, 20257.

10 R. Esfandyarpour, L. Yang, Z. Koochak, J. S. Harris and R. W. Davis, *Biomed. Microdevices*,

2016, **18**, 7.
11 C. Kirimli, W. H. Shih and W. Y. Shih, *Analyst*, 2016, **141**, 1421–1433.
12 H. T. Ngo, N. Gandra, A. M. Fales, S. M. Taylor and T. Vo-Dinh, *Biosens. Bioelectron.*, 2016, **81**, 8–14.
13 T. Wang, L. Zhou, S. Bai, Z. Zhang, J. Li, X. Jing and G. Xie, *Biosens. Bioelectron.*, 2016, **78**, 464–470.
14 Z. Zhang, J. L. Li, J. Yao, T. Wang, D. Yin, Y. Xiang, Z. Chen and G. Xie, *Biosens. Bioelectron.*, 2016, **79**, 488–494.
15 R. E. Fernandez, S. E. Williams, R. Li and A. Zhou, *Electrochem. Commun.*, 2015, **56**, 1–5.
16 H. Joda, V. Beni, I. Katakis and C. K. O'Sullivan, *Anal. Biochem.*, 2015, **474**, 66–68.
17 U. Karhunen, E. Malmi, E. Brunet, J. C. Rodríguez-Ubis and T. Soukka, *Sens. Actuators B Chem.*, 2015, **211**, 297–302.
18 Y. Zhao, H. Wang, W. Tang, S. Hu, N. Li and F. Liu, *Chem. Commun.*, 2015, **51**, 10660–10663.
19 A. Sedighi, V. Whitehall and P. C. H. Li, *Nano. Res.*, 2015, **8**, 3922–3933.
20 J. S. Wang and D. Y. Zhang, *Nat. Chem.*, 2015, **7**, 545–553.
21 D. A. Khodakov, A. S. Khodakova, D. M. Huang, A. Linacre and A. V. Ellis, *Sci. Rep.*, 2015, **5**, 8721.
22 H. Li, S. Xiao, D. Yao, M. H. W. Lam and H. Liang, *Chem. Commun.*, 2015, **51**, 4670–4673.
23 T. E. Du, X. Mao, M. Y. Jin, T. Zhang and Y. Zhang, *Sens. Actuators B Chem.*, 2014, **198**, 194–200.
24 Z. F. Gao, Y. Ling, L. Lu, N. Y. Chen, H. Q. Luo and N. B. Li, *Anal. Chem.*, 2014, **86**, 2543–2548.
25 H. Li, Z. S. Wu, Z. Shen, G. Shen and R. Yu, *Nanoscale*, 2014, **6**, 2218–2227.
26 S. Okumura, R. Kuroda and K. Inouye, *Appl. Biochem. Biotechnol.*, 2014, **174**, 494–505.
27 D. R. Sayyed, S. B. Nimse, K. S. Song and T. Kim, *Chem. Commun.*, 2014, **50**, 12344–12347.
28 A. Sedighi and P. C. H. Li, *Anal. Biochem.*, 2014, **448**, 58–64.
29 S. N. Topkaya, B. Kosova and M. Ozsoz, *Clin. Chim. Acta*, 2014, **429**, 134–139.
30 T. Song, S. Xiao, D. Yao, F. Huang, M. Hu and H. Liang, *Adv. Mater.*, 2014, **26**, 6181–6185.
31 H. Xu, W. Deng, F. Huang, S. Xiao, G. Liu and H. Liang, *Chem. Commun.*, 2014, **50**, 14171–14174.
32 W. Zhang, F. Hu, Q. Zhang, J. Zhang, Y. Mao, P. Wang and Y. Gu, *Talanta*, 2018, **179**, 685–692.
33 M. Huang, X. Zhou, H. Wang and D. Xing, *Anal. Chem.*, 2018, DOI: 10.1021/acs.analchem.7b04542.
34 Z. Zhang and I. M. Hsing, *Anal. Chem.*, 2017, **89**, 12466–12471.
35 Y. Zhang, F. Yang, Z. Sun, Y. T. Li and G. J. Zhang, *Analyst*, 2017, **142**, 3468–3476.
36 J. Xu, L. Li, N. Chen, Y. She, S. Wang, N. Liu and X. Xiao, *Chem. Commun.*, 2017, **53**, 9422–9425.
37 L. R. Wu, S. X. Chen, Y. Wu, A. A. Patel and D. Y. Zhang, *Nat. Biomed. Eng.*, 2017, **1**, 714–723.
38 M. Cui, H. Feng, D. Guo, D. Wang and B. Zheng, *Sens. Actuators B Chem.*, 2017, **253**, 731–737.
39 L. Li, X. Xiao, J. Ge, M. Han, X. Zhou, L. Wang, X. Su and C. Yu, *ACS Sens.*, 2017, **2**,

419−425.
40 X. Xiao, T. Wu, L. Xu, W. Chen and M. Zhao, *Nucleic Acids Res*., 2017, **45**, e90.
41 Q. Xu, S. Q. Huang, F. Ma, B. Tang and C. Y. Zhang, *Anal. Chem.*, 2016, **88**, 2431−2439.
42 Y. Yu, T. Wu, A. Johnson-Buck, L. Li and X. Su, *Biosens. Bioelectron.*, 2016, **82**, 248−254.
43 L. Yang, Y. Tao, G. Yue, R. Li, B. Qiu, L. Guo, Z. Lin and H. H. Yang, *Anal. Chem.*, 2016, **88**, 5097−5103.
44 A. Kausar, E. A. Osman, T. Gadzikwa and J. M. Gibbs-Davis, *Analyst*, 2016, **141**, 4272−4277.
45 S. Bi, Z. Zhang, Y. Dong and Z. Wang, *Biosens. Bioelectron.*, 2015, **65**, 139−144.
46 N. Li, Z. F. Gao, B. H. Kang, N. B. Li and H. Q. Luo, *RSC Adv.*, 2015, **5**, 20020−20024.
47 T. Wu, X. Xiao, F. Gu and M. Zhao, *Chem. Commun.*, 2015, **51**, 17402−17405.
48 T. Wu, X. Xiao, Z. Zhang and M. Zhao, *Chem. Sci.*, 2015, **6**, 1206−1211.
49 Z. K. Wu, D. M. Zhou, Z. Wu, X. Chu, R. Q. Yu and J. H. Jiang, *Chem. Commun.*, 2015, **51**, 2954−2956.
50 H. Zhang, M. Lai, A. Zuehlke, H. Peng, X. F. Li and X. C. Le, *Angew. Chem. Int. Ed.*, 2015, **54**, 14326−14330.
51 M. Drum, R. Kranaster, C. Ewald, R. Blasczyk and A. Marx, *Plos One*, 2014, **9**, e96640.
52 K. Brückner, K. Schwarz, S. Beck and M. W. Linscheid, *Anal. Chem.*, 2014, **86**, 585−591.
53 Y. He, D. Chen, M. Li, L. Fang, W. Yang, L. Xu and F. Fu, *Biosens. Bioelectron.*, 2014, **58**, 209−213.
54 J. Nie, D. W. Zhang, C. Tie, Y. L. Zhou and X. X. Zhang, *Biosens. Bioelectron.*, 2014, **56**, 237−242.
55 J. Zhu, Y. Ding, X. Liu, L. Wang and W. Jiang, *Biosens. Bioelectron.*, 2014, **59**, 276−281.

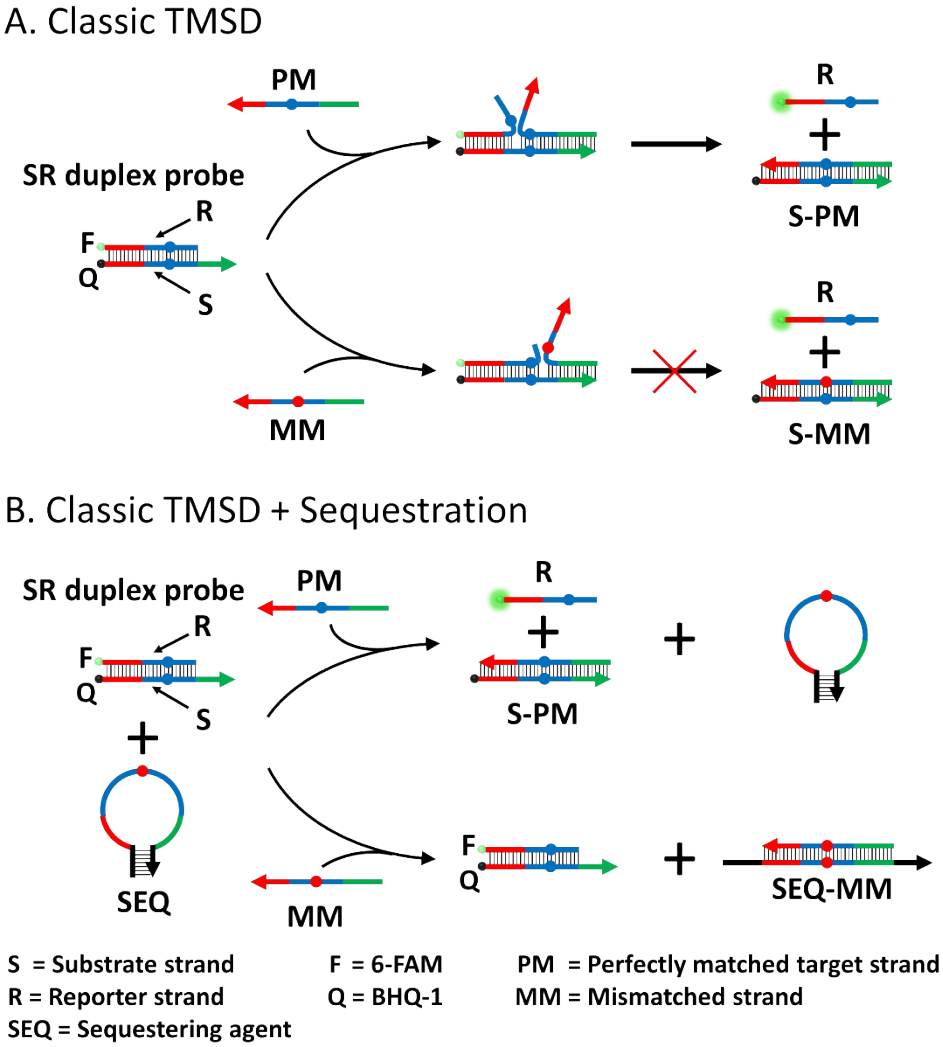

Fig. S1 Schematic representation of the SNV discrimination systems based on (A) the classic TMSD and (B) combining the classic TMSD with sequestration.

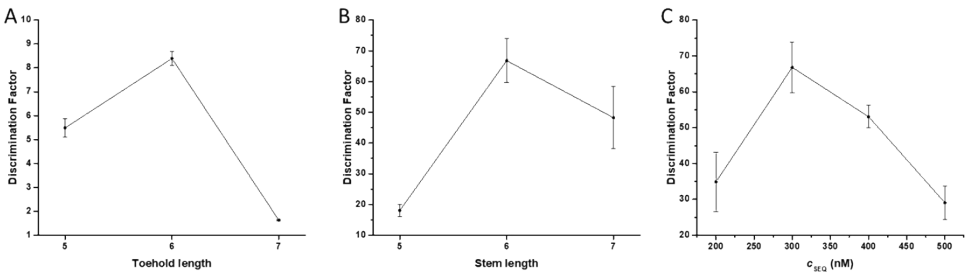

Fig. S2 Optimization of (A) the toehold length of SR duplex probe, (B) the stem length of SEQ, and (C) the SEQ concentration. The error bars represent the standard deviation of three measurements. The concentrations of SR, SEQ, PM, and MM are 20, 0, 40, and 40 nM respectively in the optimization of the toehold length, and 20, 300, 40, and 40 nM respectively in the optimization of the stem length. The concentrations of SR, PM, and MM are 20, 40, and 40 nM respectively in the optimization of the SEQ concentration.

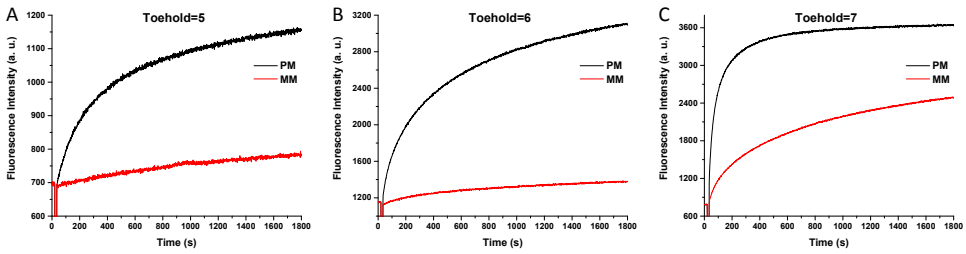

Fig. S3 Fluorescence responses of the cooperative SNV discrimination system using the SR duplex probe of different toehold lengths to PM/MM pairs of A>G substitution. The concentrations of SR, SEQ, PM, and MM are 20, 0, 40, and 40 nM, respectively.

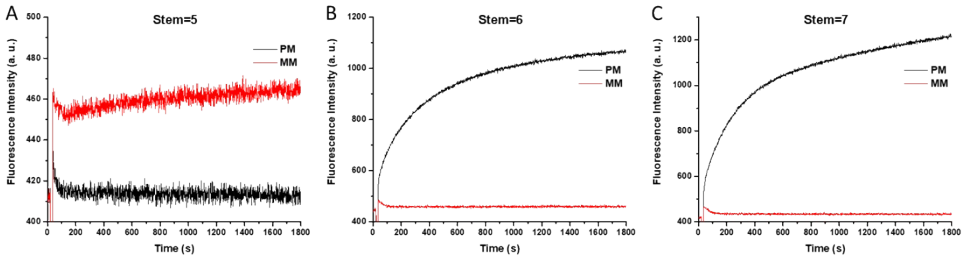

Fig. S4 Fluorescence responses of the SNV discrimination system combining cooperativity with sequestration using the SEQ of different stem lengths to PM/MM pairs of A>G substitution. The concentrations of SR, SEQ, PM, and MM are 20, 300, 40, and 40 nM, respectively.

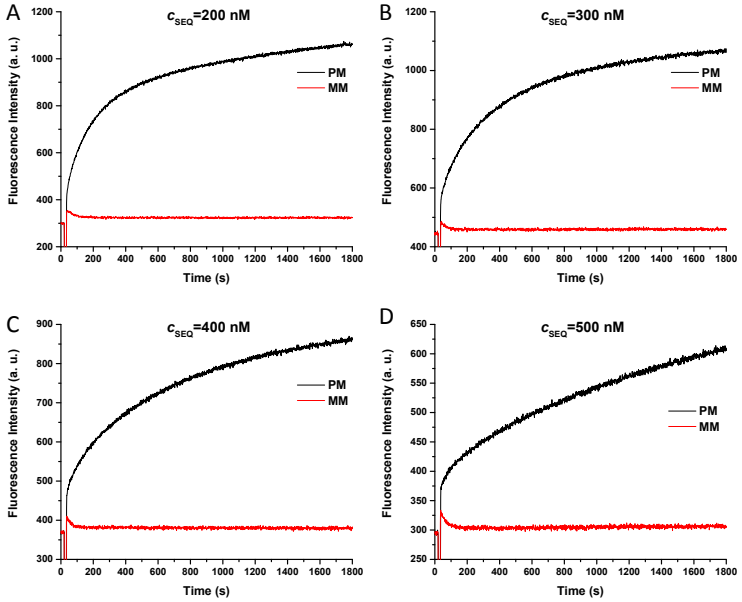

Fig. S5 Fluorescence responses of the SNV discrimination system combining cooperativity with sequestration using different SEQ concentrations to PM/MM pairs of A>G substitution. The concentrations of SR, PM, and MM are 20, 40, and 40 nM, respectively.

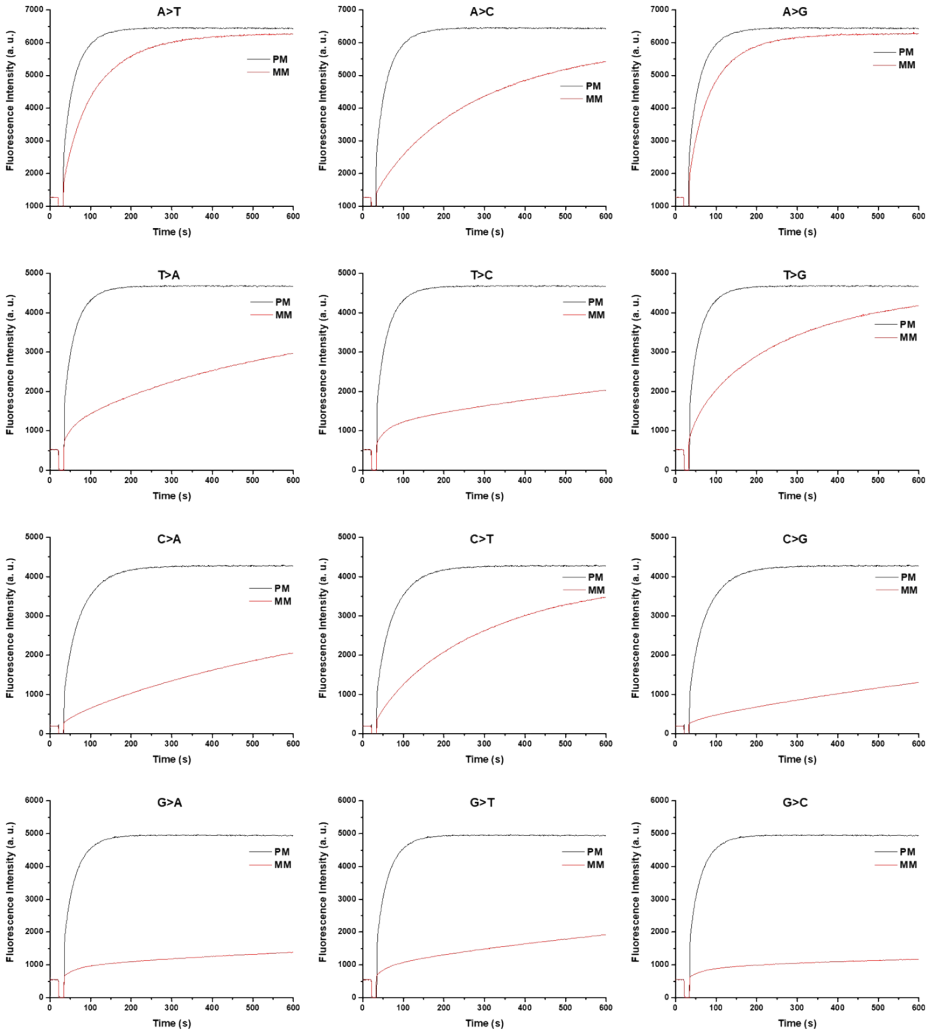

Fig. S6 Fluorescence responses of the classic TMSD system to PM/MM pairs of all 12 possible SNVs at the center position of the model sequence. The concentrations of SR, PM, and MM are 20, 20, and 20 nM, respectively.

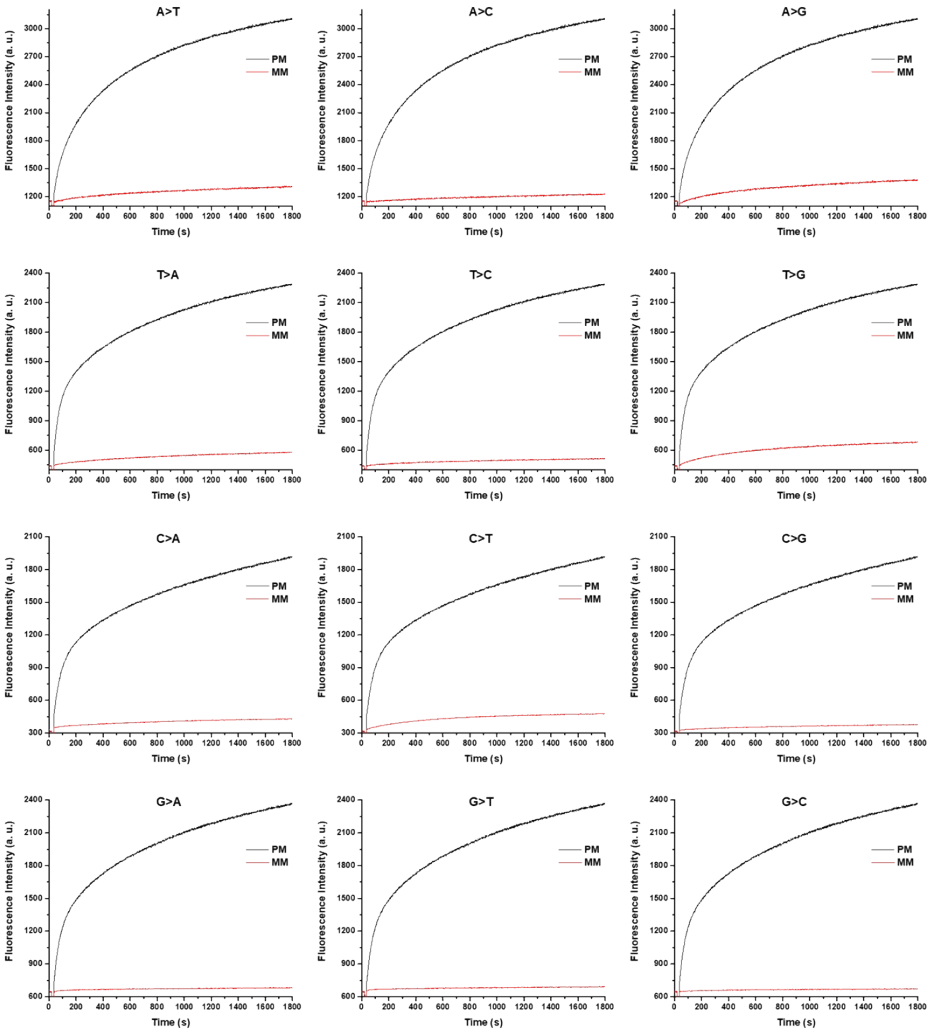

Fig. S7 Fluorescence responses of the cooperative SNV discrimination system to PM/MM pairs of all 12 possible SNVs at the center position of the model sequence. The concentrations of SR, PM, and MM are 20, 40, and 40 nM, respectively.

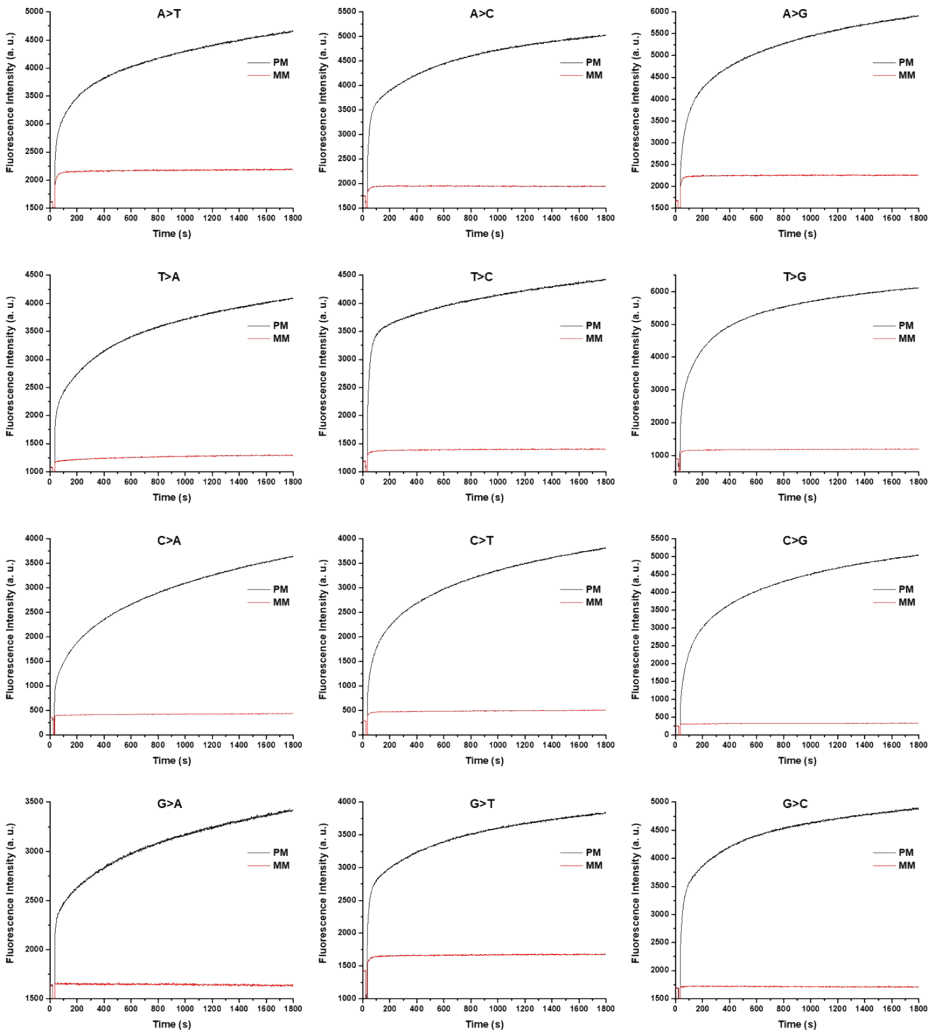

Fig. S8 Fluorescence responses of the SNV discrimination system combining the classic TMSD with sequestration to PM/MM pairs of all 12 possible SNVs at the center position of the model sequence. The concentrations of SR, SEQ, PM, and MM are 20, 300, 20, and 20 nM, respectively.

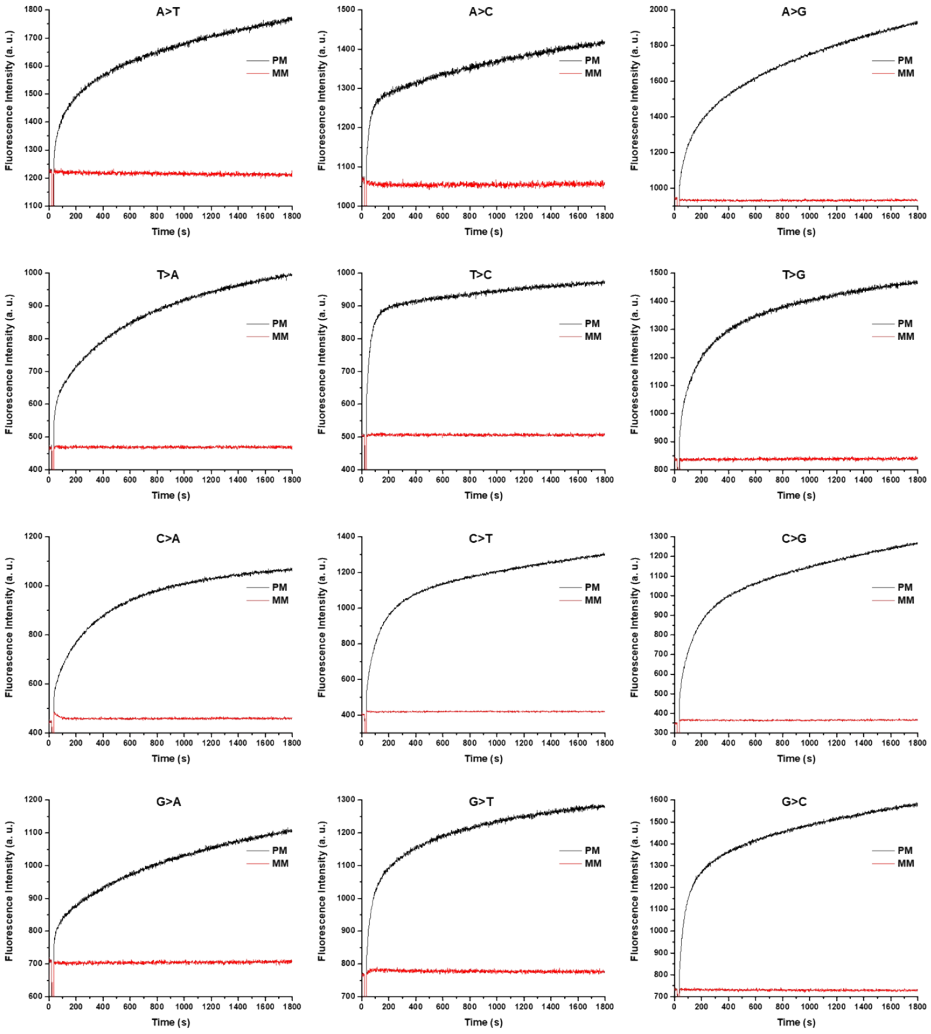

Fig. S9 Fluorescence responses of the SNV discrimination system combining cooperativity and sequestration to PM/MM pairs of all 12 possible SNVs at the center position of the model sequence. The concentrations of SR, SEQ, PM, and MM are 20, 300, 40, and 40 nM, respectively.

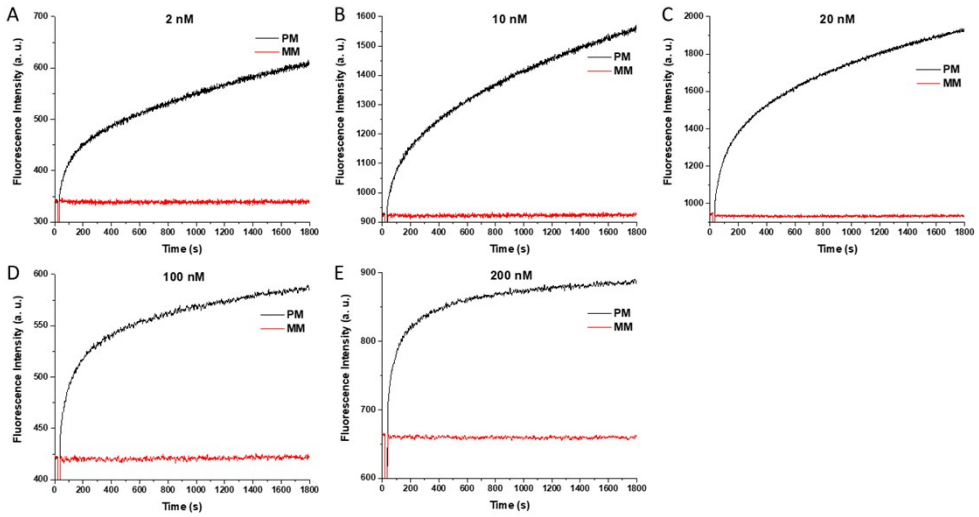

Fig. S10 Fluorescence responses of the SNV discrimination system combining cooperativity and sequestration to PM/MM pairs of A>G substitution at the center position of the model sequence using different concentrations of SR duplex probe. The concentrations of SEQ, PM, and MM are 300, 40, and 40 nM, respectively.

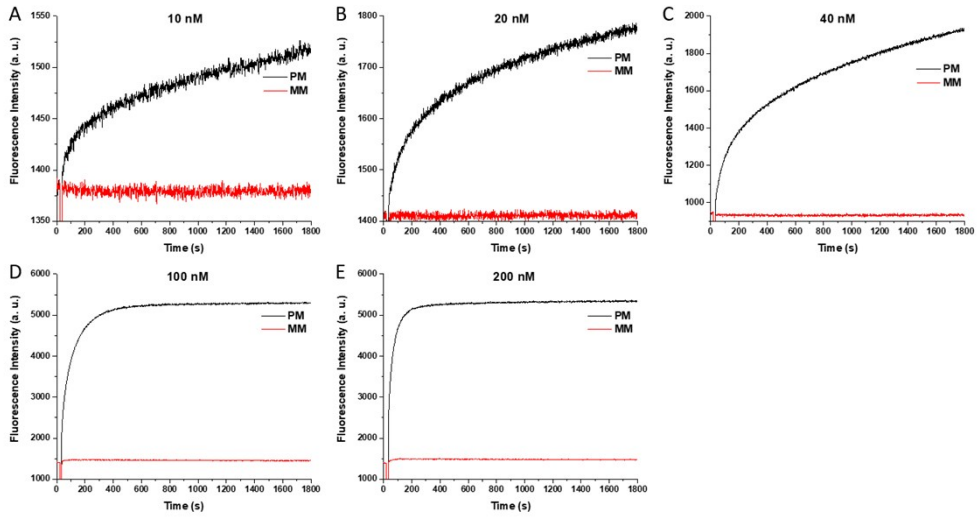

Fig. S11 Fluorescence responses of the SNV discrimination system combining cooperativity and sequestration to different concentrations of PM/MM pairs of A>G substitution at the center position of the model sequence. The concentrations of both PM and MM are the same. The concentrations of SR and SEQ are 20 and 300 nM, respectively.

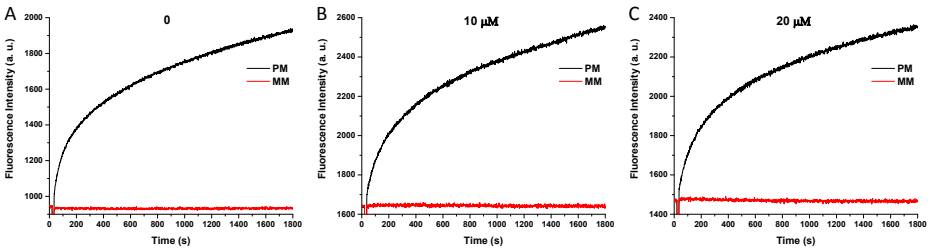

Fig. S12 Fluorescence responses of the SNV discrimination system combining cooperativity and sequestration to PM/MM pairs of A>G substitution at the center position of the model sequence in the presence of different concentrations of 50-nt random DNA sequences. The concentrations of SR, SEQ, PM, and MM are 20, 300, 40, and 40 nM, respectively.

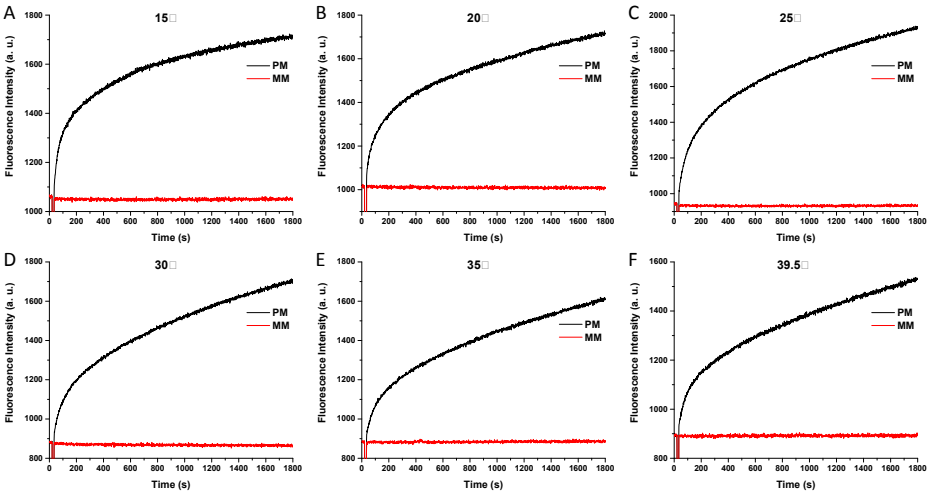

Fig. S13 Fluorescence responses the SNV discrimination system combining cooperativity and sequestration to PM/MM pairs of A>G substitution at the center position of the model sequence at different temperatures. The concentrations of SR, SEQ, PM, and MM are 20, 300, 40, and 40 nM, respectively.

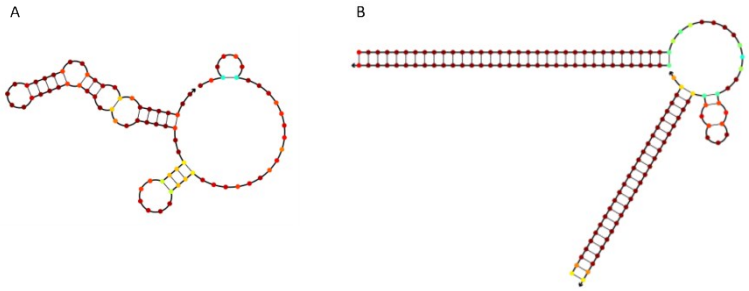

Fig. S14 The diagram of minimum free energy secondary structures (calculated using NUPACK software[1]) of (A) the PCR product alone and (B) the mixture of the PCR product and the Openers.

1 R. M. Dirks, J. S. Bois, J. M. Schaeffer, E. Winfree and N. A. Pierce, *SIAM Rev.*, 2007, **49**, 65–88.